THE JOURNAL OF BIOLOGICAL CHEMISTRY VOL. 286, NO. 20, pp. 18002–18012, May 20, 2011

Identification of Luminal Loop 1 of Scap Protein as the Sterol Sensor That Maintains Cholesterol Homeostasis*[S]

Received for publication, March 8, 2011, and in revised form, March 21, 2011 Published, JBC Papers in Press, March 24, 2011, DOI 10.1074/jbc.M111.238311

Massoud Motamed[‡1], Yinxin Zhang[‡], Michael L. Wang[‡1,2], Joachim Seemann[§], Hyock Joo Kwon[¶], Joseph L. Goldstein[‡3], and Michael S. Brown[‡]

From the Departments of [‡]Molecular Genetics, [§]Cell Biology, and [¶]Biochemistry, University of Texas Southwestern Medical Center, Dallas, Texas 75390-9046

Cellular cholesterol homeostasis is maintained by Scap, an endoplasmic reticulum (ER) protein with eight transmembrane helices. In cholesterol-depleted cells, Scap transports sterol regulatory element-binding proteins (SREBPs) to the Golgi, where the active fragment of SREBP is liberated by proteases so that it can activate genes for cholesterol synthesis. When ER cholesterol increases, Scap binds cholesterol, and this changes the conformation of cytosolic Loop 6, which contains the binding site for COPII proteins. The altered conformation precludes COPII binding, abrogating movement to the Golgi. Consequently, cholesterol synthesis declines. Here, we identify the cholesterol-binding site on Scap as Loop 1, a 245-amino acid sequence that projects into the ER lumen. Recombinant Loop 1 binds sterols with a specificity identical to that of the entire Scap membrane domain. When tyrosine 234 in Loop 1 is mutated to alanine, Loop 6 assumes the cholesterol-bound conformation, even in sterol-depleted cells. As a result, full-length Scap(Y234A) cannot mediate SREBP processing in transfected cells. These results indicate that luminal Loop 1 of Scap controls the conformation of cytosolic Loop 6, thereby determining whether cells produce cholesterol.

The endoplasmic reticulum (ER)[4] protein Scap is unique in nature because it serves as a cholesterol sensor that ensures the proper amount of cholesterol in membranes of animal cells (1, 2). The function of Scap derives from its ability to mediate the regulated transport of sterol regulatory element-binding proteins (SREBPs) from ER to Golgi. SREBPs are a family of three transcription factors that activate all of the genes necessary to produce cholesterol, fatty acids, and triglycerides (3). The SREBPs are synthesized as intrinsic transmembrane proteins of the ER. Immediately after their synthesis, the SREBPs bind to Scap, which serves as the nidus for incorporation into COPII-coated vesicles, which bud from the ER and travel to the Golgi. There the SREBPs are processed sequentially by two proteases, thereby releasing the active transcriptional fragments that travel to the nucleus. When cholesterol accumulates in ER membranes, Scap binds the cholesterol and undergoes a conformational change that causes it to bind to Insig, an ER-resident protein (4). As a result of the conformational change and its stabilization by Insig (5), the Scap-SREBP complex is no longer incorporated into budding vesicles, and the active fragment cannot reach the nucleus. As a result, synthesis of cholesterol and fatty acids declines.

The 1276 amino acids of Scap can be divided into two functional regions (see Fig. 1). The COOH-terminal domain of ~540 amino acids extends into the cytosol. It contains at least four WD repeat sequences that mediate its binding to SREBPs. The NH_2-terminal region of ~735 amino acids is the membrane attachment domain. It contains eight α-helices separated by hydrophilic loops (6). Three of the loops (Loops 1, 6, and 7) are long enough to have significant structure. Helices 2–6 contain the Insig binding site (7, 8). Loop 6, which faces the cytosol, contains the hexapeptide sequence MELADL, which serves as the binding site for the COPII proteins that cluster the Scap-SREBP complex into COPII-coated vesicles that bud from ER membranes (2, 9). When the cholesterol content of ER membranes exceeds a sharp threshold of 4–5% of total lipids, the cholesterol binds to the membrane region of Scap (10), and this elicits a conformational change in Loop 6 that can be monitored by a protease protection assay (11). The change is reflected by the exposure of a novel arginine (Arg^{505}) to cleavage by trypsin (Fig. 1).

The cholesterol-induced conformational change in Loop 6 causes the MELADL sequence to become inaccessible to COPII proteins, thereby precluding transport to the Golgi (2). Although the conformational change does not require Insig, binding to Insig stabilizes the inactive conformation, thereby lowering the threshold for cholesterol (10).

Our previous cholesterol-binding studies were performed with a recombinant form of Scap that contained the entire membrane attachment domain (TM1–8) (1, 12). Within this domain, the precise site of cholesterol binding was not established. In the current study, we localize the cholesterol-binding site to Scap Loop 1, which faces the ER lumen. We show that a point mutation in Loop 1 elicits the same conformational change in Loop 6 that is created by cholesterol binding. As a result, Scap with this point mutation cannot move from ER to Golgi, even in cholesterol-depleted cells. These studies impli-

* This work was supported in part by National Institutes of Health Grants HL20948 and GM096070.

[S] The on-line version of this article (available at http://www.jbc.org) contains supplemental Figs. S1–S3.

[1] Supported by the Ara Parseghian Medical Research Foundation.

[2] Supported by National Institutes of Health Medical Scientist Training Program Grant ST32 GM08014.

[3] To whom correspondence should be addressed: 5323 Harry Hines Blvd., Dallas, TX 75390-9046. Fax: 214-648-8804; E-mail: joe.goldstein@utsouthwestern.edu.

[4] The abbreviations used are: ER, endoplasmic reticulum; 25-HC, 25-hydroxycholesterol; HSV, herpes simplex virus; SREBP, sterol regulatory element-binding protein; TK, thymidine kinase; Tricine, *N*-[2-hydroxy-1,1-bis(hydroxymethyl)ethyl]glycine.

cate an interplay between luminal Loop 1 and cytosolic Loop 6 of Scap as a mechanism for the regulation of cholesterol metabolism in animal cells.

EXPERIMENTAL PROCEDURES

Reagents—We obtained [1,2,6,7-^{3}H]cholesterol (100 Ci/mmol) and 25-[26,27-^{3}H]hydroxycholesterol (75 Ci/mmol) from American Radiolabeled Chemicals; 24,25-epoxycholesterol and (24*S*)-hydroxycholesterol from Avanti Polar Lipids; all other sterols from Steraloids, Inc.; Nonidet P-40, FuGene 6, and Complete Protease Inhibitor Mixture from Roche Applied Sciences; Protease Inhibitor Mixture Set III and mouse anti-HSV monoclonal antibody from Novagen; trypsin (type I from bovine pancreas), monoclonal anti-green fluorescent protein (GFP), anti-c-Myc affinity gel, c-Myc peptide, and cycloheximide from Sigma; peptide *N*-glycosidase F from New England Biolabs; Fos-choline 13 from Anatrace; Ni^{2+}-NTA-agarose beads from Qiagen; cyclodextrins from Trappsol; mouse anti-His monoclonal antibody, Superdex 200 10/300 GL, Mono Q 5/50 GL, and HisTrap HP columns from GE Healthcare; gel filtration standard from Bio-Rad; rat anti-*Drosophila* hsc72 (BiP) polyclonal antibody from Babraham Institute (Cambridge, UK) (catalog no. BT-GB-1435); phRL-TK (encoding the *Renilla* luciferase gene) and Dual-Luciferase Reporter Assay System from Promega; and bovine serum albumin (catalog no. 23209) from Thermo Scientific. Complexes of cholesterol/methyl-β-cyclodextrin were prepared at a stock concentration of 2.5 mM (11). Newborn calf lipoprotein-deficient serum ($d >$ 1.215 g/ml) was prepared by ultracentrifugation (13). Solutions of compactin and sodium mevalonate were prepared as described previously (14, 15). A stock solution of 10 mM sodium oleate-bovine serum albumin in 0.15 M NaCl (final pH 7.6) was prepared as described previously (16). IgG-4H4, a mouse monoclonal antibody against hamster Scap (amino acids 1–767) (17), and IgG-9E10, a mouse monoclonal antibody against c-Myc (18), were previously described in the indicated references.

Buffers—Buffer A contained 50 mM Tris-chloride (pH 7.4), 150 mM NaCl, 1 mM dithiothreitol (DTT), and 0.005% (w/v) sodium azide. Buffer B contained 50 mM Tris-chloride (pH 7.4), 1 mM DTT, and 0.005% sodium azide. Buffer C contained 50 mM Tris-chloride (pH 7.4), 150 mM NaCl, and 0.004% Nonidet P-40. Buffer D contained 50 mM Tris-chloride (pH 7.4) and 150 mM NaCl. Buffer E contained 50 mM Tris-chloride (pH 7.5), 150 mM NaCl, 1 mM DTT, and 25 mM phosphocholine chloride. Buffer F contained 10 mM HEPES (pH 7.4), 10 mM KCl, 1.5 mM $MgCl_2$, 5 mM sodium EDTA, 5 mM sodium EGTA, and 250 mM sucrose. Buffer G contained 50 mM Tris-chloride (pH 7.4), 135 mM NaCl, 10 mM KCl, and 0.1% Nonidet P-40, and 1% (v/v) Protease Inhibitor Mixture Set III.

Culture Medium—Medium A contained a 1:1 mixture of Ham's F-12 and Dulbecco's modified Eagle's medium supplemented with 100 units/ml penicillin and 100 μg/ml streptomycin sulfate. Medium B contained medium A supplemented with 5% newborn calf lipoprotein-deficient serum, 50 μM sodium mevalonate, and 50 μM compactin, and 1% (w/v) hydroxypropyl-β-cyclodextrin. Medium C contained medium A supplemented with 5% newborn calf lipoprotein-deficient serum, 50 μM sodium mevalonate, and 50 μM compactin. Medium D contained Dulbecco's modified Eagle's medium, low glucose (1000 mg/liter) supplemented with 10% FCS, 100 units/ml penicillin, and 100 μg/ml streptomycin sulfate.

Plasmids—The pFastBacHTa expression vector encoding amino acids 1–767 of hamster Scap, referred to as His_{10}-Scap(TM1–8) (12), was modified by site-directed mutagenesis (QuikChange II XL kit, Stratagene) to generate a recombinant baculovirus designated pHis_6-Scap(Loop1). pHis_6-Scap(Loop1) encodes, in sequential order from the NH_2 terminus, the signal sequence from honeybee mellitin (19), an epitope tag consisting of six histidines, a TEV protease cleavage site (20), and luminal Loop 1 of Scap (amino acids 46–269) (see supplemental Fig. S1).

The following recombinant expression plasmids have been described: pCMV-Scap, encoding WT hamster Scap under the control of the cytomegalovirus (CMV) promoter (21); pTK-Scap, encoding WT hamster Scap under the control of the thymidine kinase (TK) promoter (22); pGFP-Scap, encoding GFP fused to WT hamster Scap under the control of the CMV promoter (23); pTK-HSV-BP2, encoding WT HSV-tagged human SREBP-2 under the control of the TK promoter (22); pTK-Insig1-Myc, encoding WT human Insig-1 followed by six tandem copies of c-Myc epitope tag under the control of the TK promoter (5); pCMV-Insig1-Myc, encoding human Insig-1 followed by six tandem copies of a c-Myc epitope tag (8); and pSRE-Luc, encoding three tandem copies of Repeat 2 + Repeat 3 of the human LDL receptor promoter, the adenovirus E1b TATA box, and the firefly luciferase gene (24). Point mutations in the above Scap plasmids were produced by site-directed mutagenesis. The coding regions of all mutated plasmids were sequenced.

Purification of His-tagged Scap(Loop1) from Sf9 Cells—On day 0, 1-liter cultures of Sf9 cells (5×10^5 cells/ml) in Sf-900 II SFM insect medium (Invitrogen) were set up at 27 °C. On day 1, cells were infected with His_6-Scap(Loop1) baculovirus. On day 3, cells were harvested and washed once with phosphate-buffered saline (PBS). The cells were then flash-frozen with liquid nitrogen and stored at −80 °C. Each pellet was resuspended in 10 pellet volumes of buffer A containing 1% (w/v) Fos-choline 13 and one Complete Protease Inhibitor Mixture tablet per 50 ml, rotated for 1 h at 4 °C, and centrifuged at $10^5 \times g$ for 1 h at 4 °C. The resulting supernatant was loaded onto a 1- or 5-ml HisTrap HP column equilibrated with 10 column volumes of buffer A containing 0.1% Fos-choline 13 and then washed sequentially with 10 column volumes of buffer A containing 0.1% Fos-choline 13 and 5 mM imidazole, followed by 25 mM imidazole. The protein was then eluted with 5 column volumes of the above buffer containing 250 mM imidazole. Peak fractions containing His_6-Scap(Loop1) were combined and concentrated with a Millipore centrifugal filter unit (10,000 molecular weight cut-off) to 1 ml and then diluted 40-fold in buffer B containing 0.1% Fos-choline 13. The resulting solution was applied to a 1-ml Mono Q column, and the protein was eluted with the above buffer containing 50 mM NaCl. The peak fractions containing His_6-Scap(Loop1) were combined, concentrated to 0.5 ml with a Millipore centrifugal filter unit (10,000 molecular weight cut-off), and then applied to a Superdex 200

10/300 GL column. His_6-Scap(Loop1) was eluted with buffer B containing 0.1% Fos-choline 13 between 12.5 and 14.5 ml, after which these fractions were combined, stored at 4 °C, and used for assays within 2 days.

[^{3}H]Cholesterol-binding Assay—All operations were carried out at room temperature. Binding reactions were set up in microcentrifuge tubes. Each reaction, in a final volume of 100 μl of buffer C with 0.004% Nonidet P-40, contained 5 pmol (150 ng) of purified His_6-Scap(Loop1) (delivered in 1 μl of buffer B containing 0.1% Fos-choline 13; final concentration in assay, 0.001%) and the indicated concentration of [^{3}H]sterol (delivered in 2 μl of ethanol) in the absence or presence of competitor sterol (delivered in 1 μl of ethanol). After incubation for 4 h at room temperature, each reaction was loaded onto a column packed with 0.3 ml of Ni^{2+}-NTA-agarose beads preequilibrated with 2 ml of buffer D. The columns were washed with 5 ml of buffer D and then eluted with 1 ml of the same buffer containing 250 mM imidazole. Aliquots of the eluate (0.7 ml) were assayed for radioactivity in a liquid scintillation counter.

[^{3}H]Cholesterol Dissociation Assay—[^{3}H]Cholesterol was prebound to His_6-Scap(Loop1) under standard assay conditions with 150 nM [^{3}H]cholesterol (see above) except that the assay was scaled up 40-fold. After incubation for 4 h at room temperature, the protein-bound [^{3}H]cholesterol was eluted from the Ni^{2+}-NTA-agarose beads in 1 ml and then diluted to a final volume of 6 ml with buffer A containing 0.1% Fos-choline 13. For the dissociation assay, the 6-ml mixture containing [^{3}H]cholesterol bound to His_6-Scap(Loop1) was divided into two aliquots of 3 ml, each of which received an addition of 24 ml of buffer C in the absence or presence of 11 μM unlabeled cholesterol. After incubation at room temperature for the indicated time, a 1-ml aliquot from each of the 27-ml sample was transferred to a tube containing 600 μl of Ni^{2+}-NTA-agarose beads. After incubation for 3 min at 4 °C, the beads were centrifuged at 800 × *g* for 1 min at room temperature, after which the supernatant was assayed for radioactivity.

Cell Culture and Transfection—SRD-13A cells, a Scap-deficient cell line derived from CHO-7 cells (25), were grown in monolayer at 37 °C in 8–9% CO_2 in medium A supplemented with 5% FCS, 1 mM sodium mevalonate, 20 mM sodium oleate-albumin, and 5 μg/ml cholesterol. SV589 cells, a line of SV-40 immortalized human fibroblasts (26), were grown in monolayer at 37 °C in 5% CO_2 in medium D. Hamster CHO-K1 cells were grown in monolayer at 37 °C and 8–9% CO_2 in medium A supplemented with 5% FCS.

Trypsin Cleavage Assay of Scap—This assay was carried out as previously described by Brown *et al.* (11) with modifications in the culture and transfection conditions. On day 0, SRD-13A cells were set up for experiments in 10 ml of medium A containing 5% FCS at a density of 8 × 10^5 cells/100-mm dish. On day 2, cells were transfected with 1 μg of full-length WT pCMV-Scap or its mutant Y234A version in 7 ml of medium A supplemented with 5% FCS; FuGENE 6 was used as the transfection agent. On day 3, the cells were washed once with PBS, harvested for preparation of membranes, and subjected to the trypsin cleavage assay (11).

Assay for Scap-Insig Complex—SRD-13A cells were set up for experiments as described above under "Trypsin Cleavage Assay of Scap" except that the cells were plated in 60-mm dishes at a density of 3 × 10^5 cells/dish. On day 2, the cells were transfected with 0.1 μg of pCMV-Insig1-Myc and 1 μg of either full-length WT pCMV-Scap or its mutant Y234A version. On day 3, the cells were switched to cyclodextrin-containing medium B. After incubation at 37 °C for 1 h, cells were washed twice with PBS and switched to medium C in the absence or presence of either 30 μM cholesterol complexed with methyl-β-cyclodextrin or 1 μg/ml 25-hydroxycholesterol (delivered in ethanol, final concentration of 0.1%). After incubation for 4 h, cells were washed twice with PBS and harvested. The pellets from three 60-mm dishes of transfected SRD-13A cells were solubilized in 1 ml of Nonidet P-40-containing buffer G, passed through a 22.5-gauge needle 15 times, and rotated for 1.5 h at 4 °C. All subsequent operations were carried out at 4 °C unless otherwise stated. The cell extracts were clarified by centrifugation at 10^5 × *g* for 30 min. Anti-Myc beads (50 μl) were added to the supernatant, followed by rotation for 16 h and centrifugation at 2000 × *g* for 1 min. The pelleted beads containing the immune complexes were washed on the rotator with 1 ml of buffer G for 30 min, followed by three additional washes in buffer G for 10 min each. The washed beads were eluted in 100 μl of buffer G with 0.25 mg/ml c-Myc peptides by rotating for 1 h at room temperature. After centrifugation at 2000 × *g* for 1 min, the supernatant was subjected to immunoblot analysis.

SREBP-2 Processing in Cultured Cells—SRD-13 cells were set up for experiments as described in the legend to Fig. 7*A*. After transfection and incubation with sterols, nuclear and membrane fractions were prepared as described previously (22) and then subjected to immunoblot analysis.

Immunoblot Analysis—Samples for immunoblotting were subjected to 10 or 13% SDS-PAGE or electrophoresis on 12% Tris-Tricine gels, after which the proteins were transferred to nitrocellulose filters that were incubated at 4 °C for 16 h with the following primary antibodies: 1 μg/ml mouse monoclonal anti-His, 1:500 dilution of a rat antiserum directed against *Drosophila* hsc72 (BiP), 1 μg/ml mouse monoclonal anti-Myc IgG-9E10, or 5 μg/ml mouse monoclonal anti-Scap IgG-4H4. Bound antibodies were visualized by chemiluminescence (SuperSignal West Pico Chemiluminescent Substrate, Thermo Scientific) using a 1:5000 dilution of anti-mouse IgG (Jackson ImmunoResearch Laboratories, Inc.) or anti-rat IgG (GE Healthcare) conjugated to horseradish peroxidase. The filters were exposed to Phoenix Research Products Blue X-ray Film (F-BX810) at room temperature.

RESULTS

Fig. 1 shows the sequence and the predicted topology of the membrane domain of Scap as deduced in previous studies (6). This segment has eight transmembrane helices and three loops that are large enough to have secondary structure. Loop 1 comprises 245 amino acids and faces the lumen. It contains a site for *N*-linked glycosylation near its C terminus. Loop 6, which faces the cytosol, was shown previously to contain the sequence MELADL, which is the binding site for COPII proteins that carry the Scap-SREBP complex from ER to Golgi (2, 9). Loop 7, which faces the lumen, contains an epitope that allows immunodetection of a tryptic fragment that changes in response to a

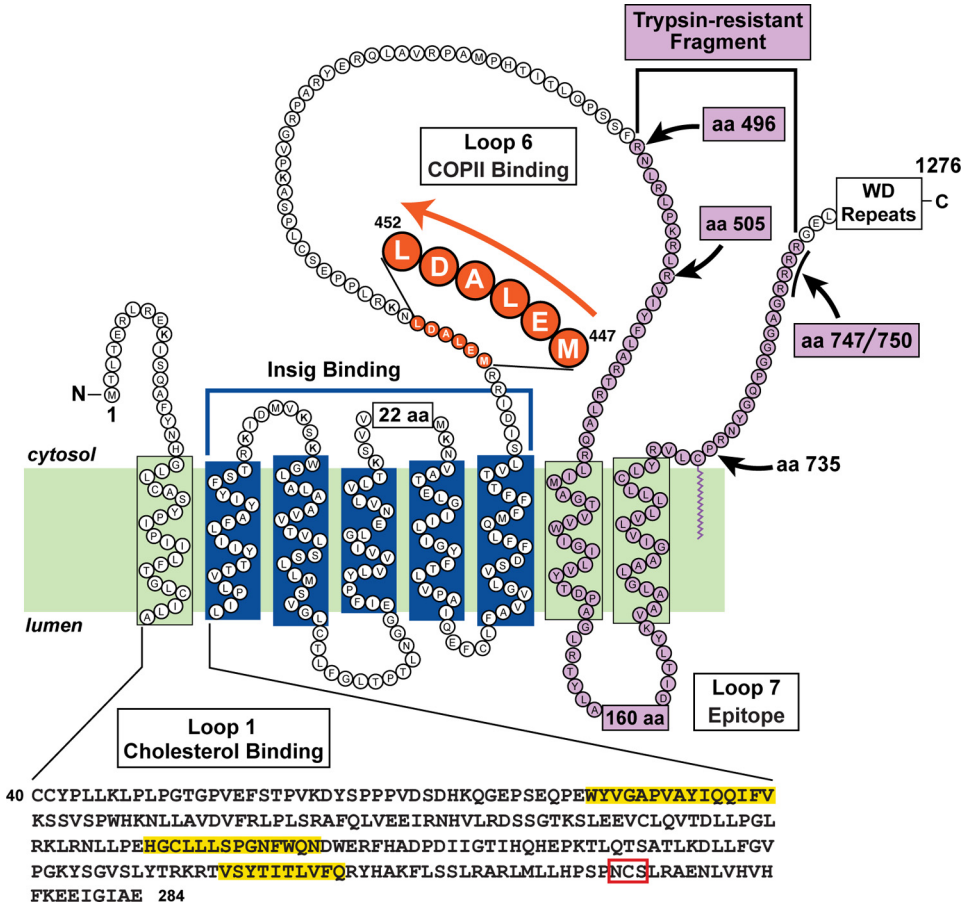

FIGURE 1. **Topology model of the membrane region of hamster Scap, showing its three functional domains.** The cholesterol-binding domain is localized to luminal Loop 1; the three hydrophobic patches in its amino acid (*aa*) sequence are *shaded* in *yellow*, and the *N*-linked glycosylation site is denoted by the *red box*. The Insig-binding domain is localized to transmembrane helices 2–6, shown by the *blue bracket*. The COPII-binding site is localized to the MELADL sequence in Loop 6, *shaded* in *red*. Amino acids 496–747/750 (shaded in *purple*) correspond to the trypsin-resistant fragment generated by a sterol-regulated conformational change in Scap.

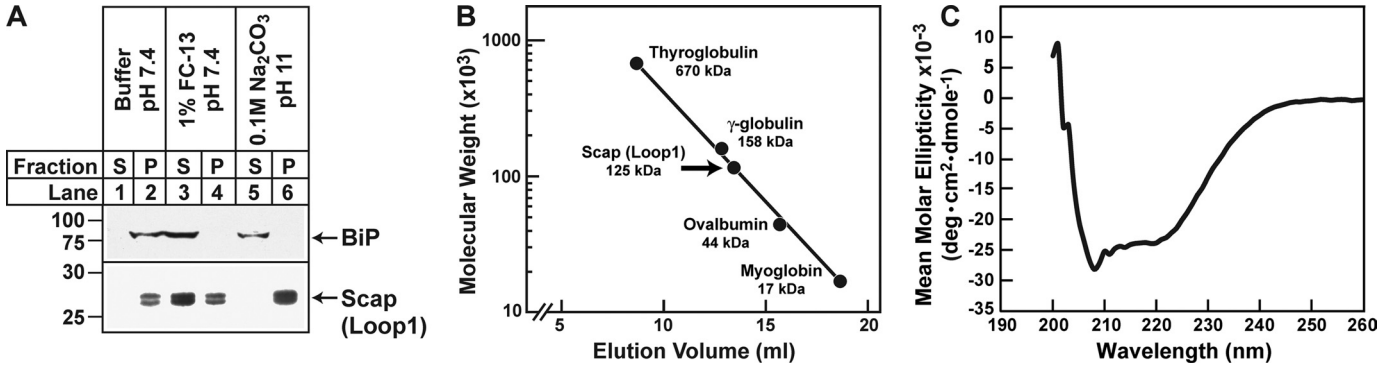

FIGURE 2. **Biochemical properties of His_6-Scap(Loop1).** *A*, membrane attachment. Aliquots of baculovirus-infected Sf9 cell pellets (representing ~2×10^5 cells) were each homogenized in 0.5 ml of one of the following buffers: 50 mM Tris-chloride (pH 7.4) and 100 mM NaCl (*lanes 1* and *2*); buffer A with 1% Fos-choline 13 (*lanes 3* and *4*); or 100 mM sodium carbonate at pH 11 (*lanes 5* and *6*). After rotating for 2 h at 4 °C, the samples were centrifuged at $10^5 \times g$ for 30 min at 4 °C, after which the resulting pellets were solubilized in 0.5 ml of 10 mM Tris at pH 7.4, 100 mM NaCl, and 1% SDS. Aliquots of the supernatant (*S*) and pellet (*P*) were subjected to 13% SDS-PAGE and immunoblot analysis with anti-His (Scap(Loop1)) or anti-BiP. Films were exposed for 8–10 s. *B*, molecular weight determination. Buffer A containing 0.1% Fos-choline 13 and either gel filtration standards or 125 μg of His_6-Scap(Loop1) were loaded in a final volume of 0.5 ml onto a Superdex 200 10/300 GL column and chromatographed at a flow rate of 0.5 ml/min. Positions of elution of the gel filtration standards and His_6-Scap(Loop1) were identified by monitoring absorbance at 280 nM and immunoblotting with anti-His, respectively. *C*, circular dichroism spectroscopy. Spectroscopic measurements of 3 μM His_6-Scap(Loop1) in buffer A containing 0.1% Fos-choline 13 were carried out in an Aviv 62DS spectrometer using a 2-mm path length cuvette. The mean of four spectra for each curve is shown.

sterol-induced conformational change in the structure of Loop 6 (2, 11).

We prepared a baculovirus encoding nearly the entire Loop 1 (residues 46–269) preceded by a cassette composed of the signal sequence from honeybee mellitin followed by six histidines and a tobacco etch virus protease cleavage site (supplemental Fig. S1). After introduction into insect cells, the cells produced Loop 1 as a membrane-attached protein (Fig. 2*A*, *lanes 1* and *2*).

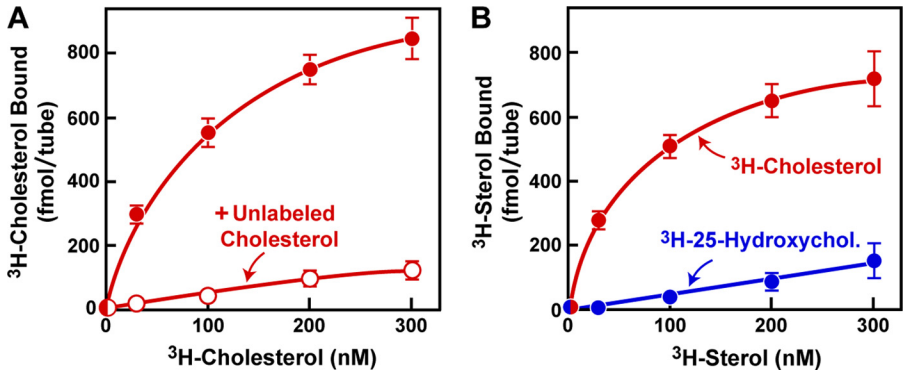

FIGURE 3. **[^{3}H]Sterol binding to His$_6$-Scap(Loop1).** Each reaction, in a final volume of 100 μl of buffer C with 0.004% Nonidet P-40 and 0.001% Fos-choline 13, contained 5 pmol of purified His$_6$-SCAP(Loop1), 1 μg of bovine serum albumin, and the indicated concentration of either [^{3}H]cholesterol (222 dpm/fmol) or 25-[^{3}H]hydroxycholesterol (165 dpm/fmol) in the absence (●) or presence (○) of 10 μM unlabeled sterol, as indicated. After 4 h at room temperature, the bound [^{3}H]sterol was measured as described under "Experimental Procedures." Each data point denotes the mean ± S.E. of triplicate assays. *A*, total [^{3}H]cholesterol binding without subtraction of blank values. *B*, specific [^{3}H]cholesterol or 25-[^{3}H]hydroxycholesterol binding after subtraction of blank values determined in the presence of the respective unlabeled sterol at 10 μM (<127 fmol/tube for [^{3}H]cholesterol binding; <30 fmol/tube for 25-[^{3}H]hydroxycholesterol binding).

No detectable amounts of Loop 1 were secreted into the medium. Membrane-bound Loop 1 showed two bands upon SDS-PAGE. NH_2-terminal sequencing by Edman degradation revealed that the upper band represents protein that retains the signal sequence because it has not been cleaved by signal peptidase. The lower band contains protein that was processed by signal peptidase. Treatment with tobacco etch virus protease reduced both proteins to a single band (data not shown). Both forms of the protein could be solubilized from the membrane by treatment with a detergent (Fos-choline 13) (Fig. 2*A*, *lanes 3* and *4*), but neither one was released by treatment with Na_2CO_3 at pH 11 (Fig. 2*A*, *lanes 5* and *6*), indicating that Loop 1 is attached to the membrane by hydrophobic forces. The detergent-solubilized protein was purified by sequential chromatography on a nickel column and an ion exchange column, followed by gel filtration. Upon gel filtration in 0.1% Fos-choline 13, the protein had an apparent molecular mass of 125 kDa (Fig. 2*B*), consistent with a tetramer. Circular dichroism indicated a largely helical structure (Fig. 2*C*).

Sterol-binding studies were performed with preparations of purified Scap Loop 1 that contained molecules with and without the signal sequence. To measure cholesterol binding, we incubated the recombinant protein with [^{3}H]cholesterol in buffer containing 0.004% Nonidet P-40 and 0.001% Fos-choline 13. The mixture was applied to a nickel column that was washed without detergent, and the protein-bound [^{3}H]cholesterol was eluted with 250 mM imidazole in detergent-free buffer and quantified by scintillation counting. As shown in Fig. 3, recombinant Loop 1 bound [^{3}H]cholesterol with saturation kinetics (calculated K_d = 67 nM), which is comparable with the apparent K_d of 50–100 nM when the binding studies were performed with the entire membrane attachment domain (TM1–8) (12). In the presence of an excess of unlabeled cholesterol, [^{3}H]cholesterol dissociated from Loop 1 with a half-time of ~10 min (supplemental Fig. S2*B*). This dissociation rate is similar to that previously shown for Scap(TM1–8) (see Fig. 4 of Ref. 12). The dissociation of [^{3}H]cholesterol resulted from exchange with unlabeled cholesterol, as indicated by the lack of dissociation in the absence of cholesterol (supplemental Fig. 2*B*). Like the entire membrane domain of Scap (12), Loop 1 did not bind 25-[^{3}H]hydroxycholesterol in a saturable fashion (Fig. 3*B*).

To analyze the sterol specificity of Loop 1 binding, we performed competition studies with various unlabeled sterols. Androstenol and desmosterol competed as well as cholesterol for [^{3}H]cholesterol binding, whereas epicholesterol, lanosterol, and 25-hydroxycholesterol did not compete (Fig. 4*A*). Fig. 4*B* compares the ability of 21 sterols at 1.5 μM to compete for [^{3}H]cholesterol binding to Loop 1. For comparative purposes, Fig. 4*C* is replotted from Fig. 3*D* of Radhakrishnan *et al.* (1), who studied sterol competition for [^{3}H]cholesterol binding to the entire transmembrane region of Scap, designated Scap(TM1–8). The sterols are grouped into effective competitors (shown in *red*), partial competitors (shown in *blue*), and non-competitors (shown in *black*). The sterol specificity of Loop 1 coincides precisely with that of the entire transmembrane domain.

We next carried out alanine-scanning mutagenesis of Loop 1 to identify functional residues. Single residues or clusters of 2 or 3 contiguous residues were changed to alanine in a plasmid that encodes full-length Scap under control of the herpes simplex TK promoter. The mutant plasmids were introduced into hamster SRD-13A cells, a mutant CHO cell line that lacks Scap (25), together with plasmids encoding firefly luciferase under control of an SRE-containing promoter and Insig-1 under control of the TK promoter. To control for transfection efficiency, we included a plasmid encoding *Renilla* luciferase, also under control of the TK promoter. The cells were depleted of cholesterol by incubation with hydroxypropyl-β-cyclodextrin, and some of the cells were repleted by the addition of cholesterol complexed with methyl-β-cyclodextrin. The cells were harvested, and the ratio of firefly to *Renilla* luciferase was measured. In cells that received no Scap, there was little firefly luciferase activity (Fig. 5*A*). WT Scap led to high luciferase activity that was reduced by 80% in the presence of cholesterol. Several of the mutant plasmids showed no luciferase activity in the absence of cholesterol (indicated by *red asterisks* in Fig. 5*A*). We hypothesized that these mutations impaired the ability of Scap to carry SREBPs to the Golgi complex.

To deconvolute the cluster mutations that appeared to abolish Scap activity, we prepared additional plasmids in which each of the residues in each cluster was changed individually to alanine (Fig. 5*B*). These data revealed two single amino acid substitutions that abolished Scap transport activity. These were

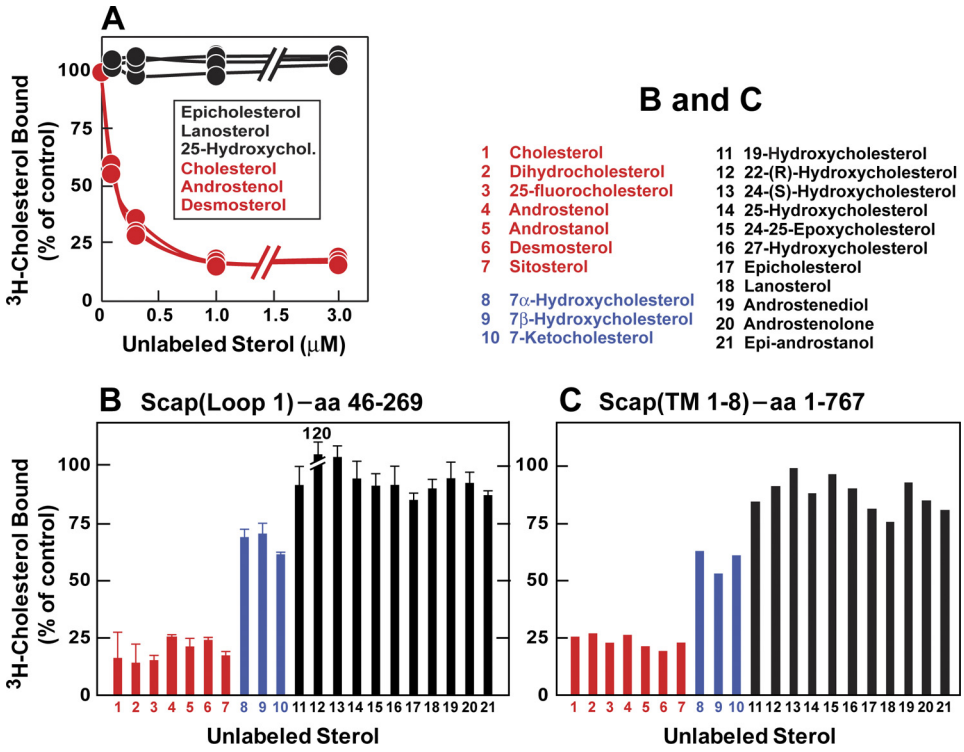

FIGURE 4. **Comparison of the sterol specificity of [^{3}H]cholesterol binding to Scap(Loop1) and Scap(TM1–8).** *A* and *B*, competitive binding of unlabeled sterols to His_6-Scap(Loop1). Each reaction, in a final volume of 100 μl of buffer C with 0.004% Nonidet P-40 and 0.001% Fos-choline 13, contained 5 pmol of His_6-Scap(Loop1), 1 μg of bovine serum albumin, 150 nM [^{3}H]cholesterol (222 dpm/fmol), and either varying concentrations of the indicated unlabeled sterol (*A*) or a 1.5 μM concentration of the indicated unlabeled sterol (*B*). After 4 h at room temperature, bound [^{3}H]cholesterol was measured by the Ni^{2+}-NTA-agarose assay, as described under "Experimental Procedures." Each value represents total binding without subtraction of blank values and is the average of duplicate (*A*) or triplicate (*B*) assays. The "100% of control" values, determined in the absence of unlabeled sterols, was 398 fmol/tube and 673 fmol/tube in *A* and *B*, respectively. *C*, competitive binding of unlabeled sterols to His_{10}-Scap(TM1–8). These data are replotted from Fig. 3*D* of Radhakrishnan *et al.* (1). Briefly, each assay tube, in a final volume of 100 μl of buffer E with 0.1% Fos-choline 13, contained 120 nM His_{10}-Scap(TM1–8), 100 nM [^{3}H]cholesterol (120 dpm/fmol), and a 5 μM concentration of the indicated sterol. After 4 h at room temperature, the amount of bound [^{3}H]cholesterol was determined by the Ni^{2+}-NTA-agarose assay. The "100% of control" values, determined in the absence of unlabeled sterols, ranged from 209 to 263 fmol/tube. No blank values were subtracted. Each data point is the average of duplicate assays. *aa*, amino acids.

V98A and Y234A. We chose the Y234A mutant for further study.

To confirm visually the lack of movement of Scap(Y234A) to the Golgi, we introduced the Y234A mutation into a plasmid encoding a fusion protein between Scap and GFP (Fig. 6). Cells were depleted of sterols and then fixed and permeabilized for fluorescence microscopy. Scap was visualized by virtue of its GFP tag. The Golgi complex was visualized by incubation with an antibody directed against Golgi protein GM130, followed by an anti-immunoglobulin coupled to a red Alexa dye. Nuclei were stained with Hoechst dye (blue). Under these conditions, WT Scap-GFP was concentrated in the Golgi, where it co-localized with GM130 (Fig. 6, *upper panels*). In contrast, the vast majority of Scap(Y234A) was found in a lacy pattern corresponding to ER, and there was no specific localization to the Golgi (Fig. 6, *bottom panels*). The images shown in Fig. 6 are representative of many transfected cells that were examined individually ($n = 79$ WT; $n = 70$ mutant).

To confirm that the Y234A mutation abolishes the ability of Scap to facilitate SREBP processing, we transfected plasmids encoding WT or Y234A mutant Scap into Scap-deficient SRD-13A cells (Fig. 7*A*). Some of the cells also received a plasmid encoding Myc-tagged Insig-1. The cells were depleted of sterols, and some were repleted with cholesterol or 25-hydroxycholesterol (25-HC). Nuclear extracts and membrane pellets were isolated and subjected to SDS-PAGE. In the absence of co-transfection with Insig-1, overexpression of WT Scap caused the appearance of the nuclear fragment of SREBP-2 (*lane 2*), and there was minimal reduction when cholesterol or 25-HC was added (*lanes 3* and *4*). When Insig-1 was overexpressed together with WT Scap, the nuclear fragment of SREBP-2 was seen in sterol-depleted cells (*lane 5*), and the fragment disappeared when cholesterol or 25-HC was present (*lanes 6* and *7*). When cells expressed Scap(Y234A), nuclear SREBP-2 was barely detectable in the absence or presence of sterols, and Insig-1 had no further inhibitory effect (*lanes 8–13*). Immunoblotting with anti-Scap confirmed the equal expression of WT and Y234A mutant Scap after transfection (*lanes 2–13*, Scap immunoblot).

To learn the reason for the defective behavior of Scap(Y234A), we introduced the mutation into a baculovirus encoding His-tagged Scap(Loop1), and we purified the mutant loop together with WT Loop 1 as described above. Both mutant and WT Loop 1 bound [^{3}H]cholesterol with similar affinity (Fig. 7*B*). Fig. 7*C* shows the trypsin cleavage assay that we used previously to demonstrate a sterol-induced conformational change in Loop 6 of Scap (2, 11) (see Fig. 1). Cells were transfected with plasmids encoding full-length WT Scap or the Y234A mutant. A 20,000 × *g* pellet of sealed vesicles was isolated and incubated with or without cholesterol complexed to

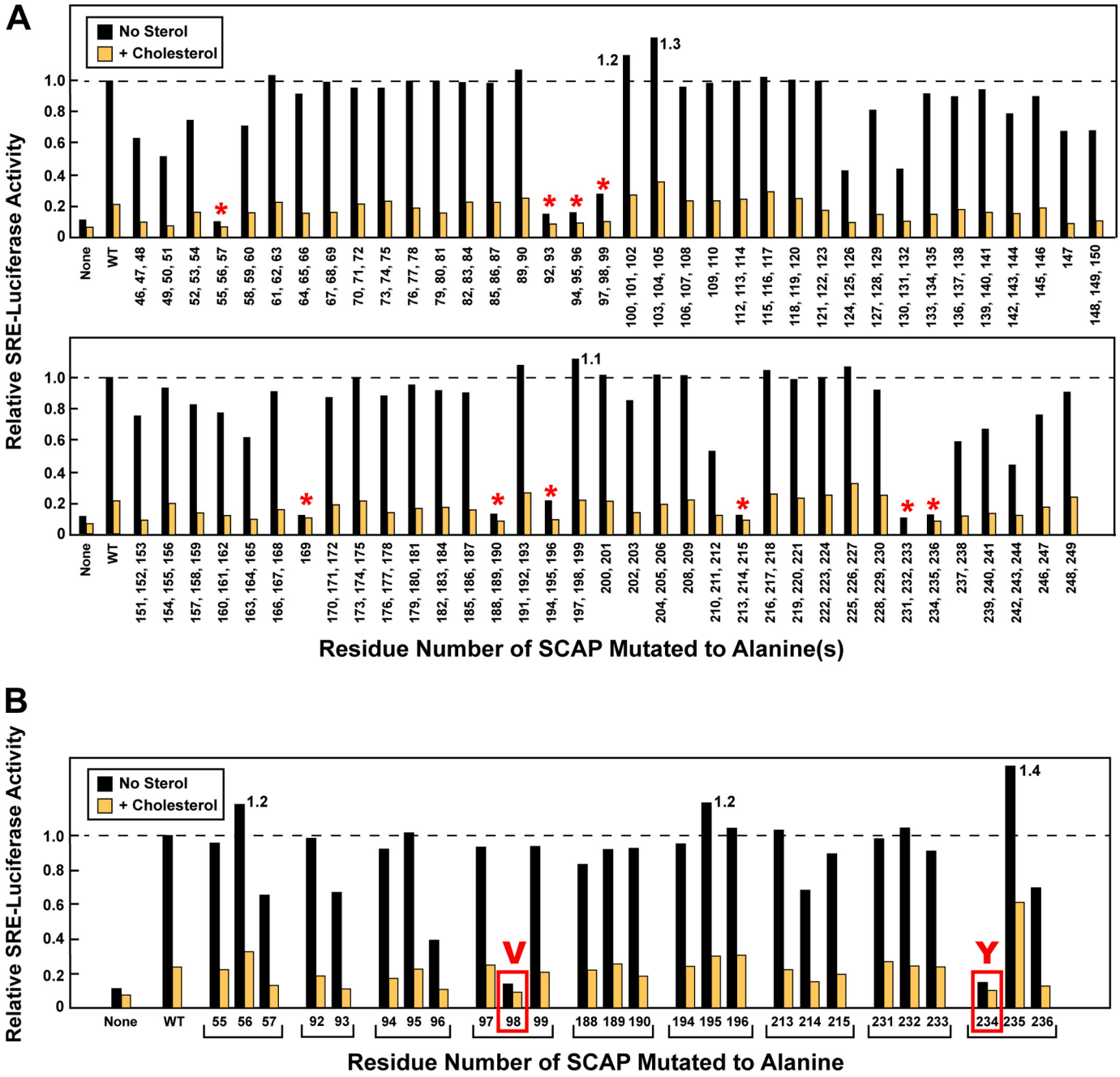

FIGURE 5. **Alanine-scanning mutagenesis of Loop 1 region of hamster Scap.** *A* and *B*, on day 0, SRD-13 cells were set up for experiments in 1 ml of medium A containing 5% FCS at a density of 3×10^4 cells/well in 24-well plates. On day 1, cells were cotransfected in 1 ml of medium A supplemented with 5% FCS containing 38 ng of pTK-Insig1-Myc, 125 ng of pSRE-firefly luciferase, 125 ng of pTK-*Renilla* luciferase, and 50 ng of WT pTK-Scap or the indicated mutant pTK-Scap in which 1–3 residues were mutated to alanine. FuGENE 6 was used as the transfection agent. For each transfection, the total amount of DNA was adjusted to 338 ng/dish by the addition of pcDNA mock vector. On day 2 (after incubation with plasmids for 24 h), the cells were washed once with PBS and then treated with hydroxypropyl-β-cyclodextrin-containing medium B for 1 h. Cells were then washed twice with PBS and refed with 1 ml of medium C in the absence or presence of 15 μM cholesterol complexed with methyl-β-cyclodextrin. After incubation for 16 h, the cells were washed with PBS, after which luciferase activity was read on a Synergy 4 plate reader (BioTek) according to the Promega protocol. The amount of SRE-firefly luciferase activity in each dish was normalized to the amount of *Renilla* luciferase activity in the same dish. Relative SRE-luciferase activity of 1.0 represents the normalized luciferase value in dishes transfected with WT pTK-Scap in the absence of cholesterol. All values are the average of duplicate assays. *A*, *red asterisks* denote single, double, or triple contiguous alanine mutations that produced a loss of SRE-luciferase activity in both the absence and presence of cholesterol. The data in these graphs were obtained in four different experiments, each with its own WT control. *B*, deconvolution of double or triple mutants that showed loss of SRE-luciferase activity in *A*. *Red boxes* denote single alanine mutations that continued to show loss of SRE-luciferase activity. Each value is the average of duplicate assays.

methyl-β-cyclodextrin. The membranes were then treated with trypsin, after which the proteins were subjected to Tris-Tricine gel electrophoresis and blotted with an antibody against an epitope in Loop 7 that faces the lumen and is thus protected from trypsin (see Fig. 1). In sterol-depleted membranes, trypsin cleaves Loop 6 at arginine 496 and arginines 747–750, which produces a fragment of 250 amino acids that corresponds to the band seen in Fig. 7*C*, *lane 1*. After incubation with cholesterol, arginines 503 and 505 become exposed to trypsin. Cleavage at these sites produces a fragment of ~241 amino acids, which

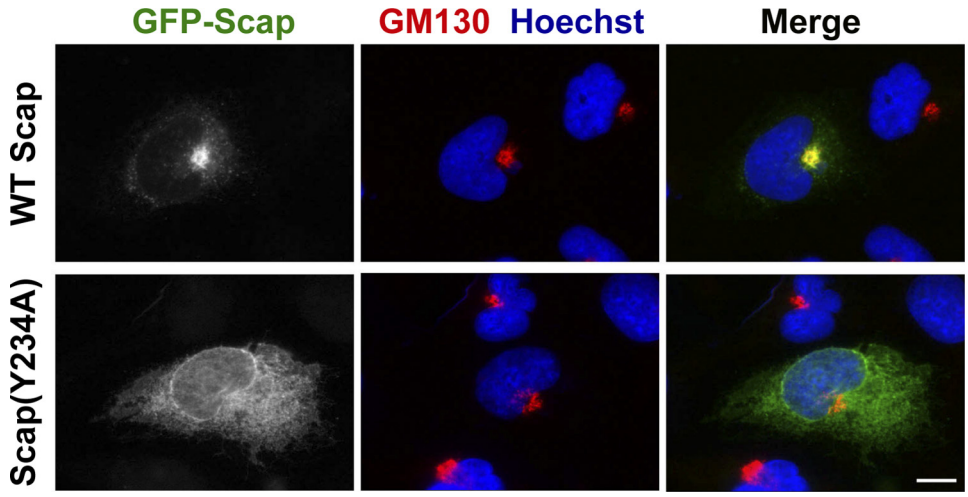

FIGURE 6. **ER-to-Golgi transport of WT and Y234A mutant version of GFP-Scap.** On day 0, SV589 cells were set up for experiments in medium D at a density of 1×10^5 cells/37-mm dish containing three 12-mm glass coverslips. On day 1, cells were transfected with 1 μg of full-length WT pGFP-Scap (*top panels*) or its mutant Y234A version (*bottom panels*) in 3 ml of medium A supplemented with 5% FCS. FuGENE 6 was used as the transfection reagent. On day 2, the cells were washed once with PBS and then incubated for 1 h at 37 °C with cyclodextrin-containing medium B supplemented with 50 μg/ml cycloheximide, after which each coverslip was fixed, permeabilized in methanol at −20 °C for 15 min, and then incubated with 0.625 μg/ml monoclonal antibody against the Golgi-resident protein GM130 (BD Biosciences), followed by 6.7 μg/ml goat anti-mouse antibodies conjugated to Alexa 594 (Invitrogen). The nuclei were then stained with 1 μg/ml Hoechst 33342 (Invitrogen), and the coverslips were mounted in Mowiol 4-88 (Calbiochem) mounting solution (35). Fluorescence images were acquired using an LD Plan-Neofluar ×40/1.3 differential interference contrast objective, an Axiovert 200 M microscope (Zeiss), an Orca 285 camera (Hamamatsu), and the software Openlab 4.0.2 (Improvision). *Scale bar*, 10 μm.

corresponds to the lower band (*lane 3*). The Y234A mutant of Scap showed substantial amounts of the lower band, even in cholesterol-depleted membranes (*lane 2*). There was a further reduction in the upper band when cholesterol was added (*lane 4*). These data indicate that Loop 6 in the Y234A mutant is largely in the cholesterol-bound conformation even in sterol-depleted membranes.

When Scap is in the cholesterol-bound conformation, the protein binds to Insig, which stabilizes the cholesterol-bound conformation (7). Fig. 7*D* shows an experiment designed to determine whether Scap(Y234A) binds to Insig-1 in sterol-depleted cells, as determined by an Insig-1 co-immunoprecipitation assay. Scap-deficient SRD-13A cells were co-transfected with plasmids encoding Myc-tagged Insig-1 and either WT Scap or the Y234A mutant. The cells were depleted of cholesterol, and some were repleted with cholesterol or 25-HC. Detergent extracts were prepared, and Insig-1 was precipitated with anti-Myc. After SDS-PAGE the precipitates were probed with antibodies against Scap and Insig-1. In sterol-depleted cells, WT Scap did not co-precipitate with Insig-1 (Fig. 7*D*, *lane 1*). The addition of cholesterol (*lane 2*) or 25-HC (*lane 3*) caused Scap to be co-precipitated. In contrast, Scap(Y234A) was co-precipitated with Insig-1 even in the absence of sterol (*lane 4*). There was a slight increase when 25-HC was added (*lane 6*). In the immunoblots in this experiment, we noted that Scap showed two bands. We believe that the upper band represents an SDS-resistant dimer that forms when Scap has been incubated in detergents for prolonged periods, as required for the co-immunoprecipitation experiment. Insig-1 also appears as a doublet, due to the presence of two initiator methionines (7).

DISCUSSION

The studies in this paper identify Loop 1 of Scap as a crucial component of the cholesterol-sensing mechanism in animal cells. When examined *in vitro*, this loop binds sterols with specificity that is identical to that of the whole membrane attachment domain (TM1–8). Moreover, a point mutation in Loop 1 (Y234A) converts Loop 6 of Scap constitutively into the cholesterol-bound conformation, as monitored by the protease protection assay. Consistent with this observation, Scap(Y234A) binds to Insig even in sterol-depleted cells, and it cannot transport SREBP-2 to the Golgi, even after sterol depletion. These findings are consistent with the protease protection assay and suggest that the MELADL sequence in Scap(Y234A) is unable to interact with COPII proteins. Precisely how a change in Loop 1 causes a change in Loop 6 is not known, but the current findings establish this interplay as a crucial element in the regulation of cholesterol metabolism in animal cells.

The way in which a luminal loop of Scap binds intramembrane cholesterol remains to be determined. When expressed in insect cells, this loop is bound tightly to membranes, most likely ER membranes. The protein cannot be released by chaotropic agents, and it requires detergents for extraction. Loop 1 contains three hydrophobic segments, as indicated in *yellow* in Fig. 1. None of these has the characteristics of a membrane-spanning helix, as determined by hydrophobicity plots (see Fig. 1 of Ref. 6). The evidence that Loop 1 lies in the ER lumen is based on studies of the glycosylation site at amino acid 263 in this loop (Fig. 1). This sequence was shown to be glycosylated when full-length Scap was produced in CHO cells (6). It seems likely that the hydrophobic segments in Loop 1 dip into the membrane but do not cross it. Within the membrane, these segments would be in a position to bind intramembrane cholesterol.

Our alanine-scanning mutagenesis failed to identify residues that are crucial for cholesterol binding, as indicated by the SRE-

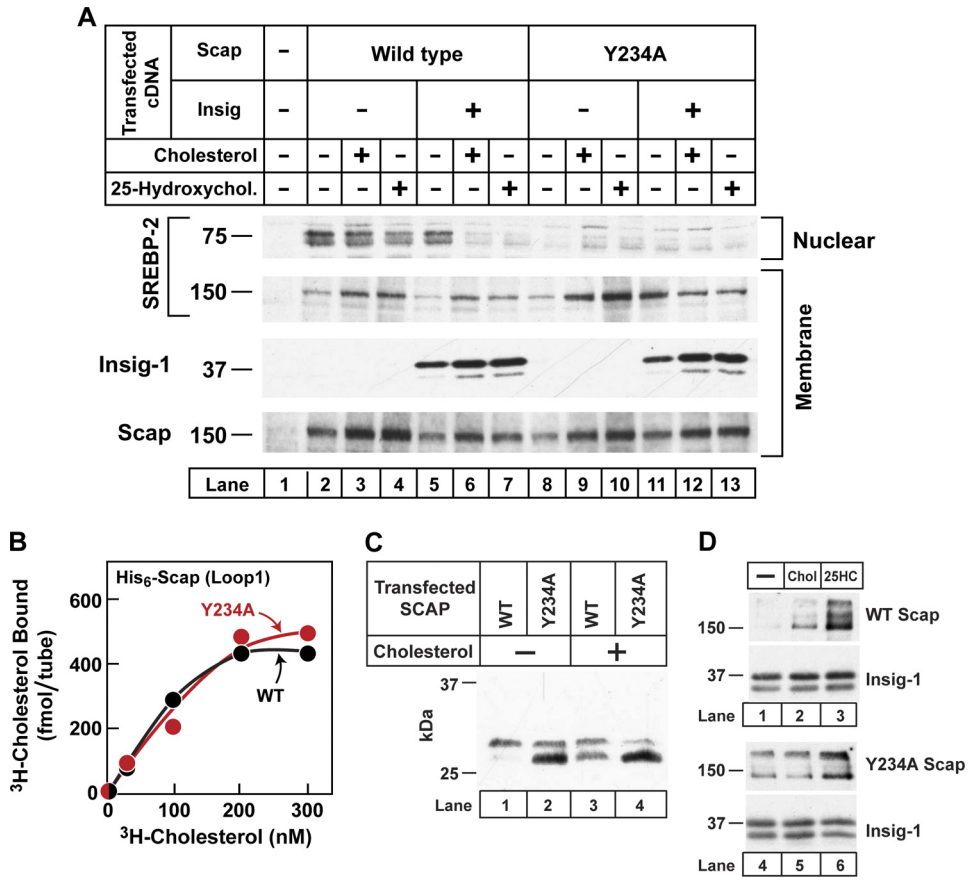

FIGURE 7. **Biochemical characterization of the Y234A mutant Scap.** *A*, immunoblot analysis of SREBP-2 in Scap-deficient cells transfected with WT or Y234A mutant version of full-length Scap in the absence or presence of transfected Insig-1. On day 0, SRD-13A cells were set up for experiments at a density of 3×10^5 cells/60-mm dish in 4 ml of medium A containing 5% FCS. On day 2, cells were transfected with 2 μg of TK-HSV-BP2 and 0.4 μg of full-length pTK-Scap (WT or its Y234A mutant) with or without 0.3 μg of pTK-Insig 1-Myc in 7 ml of medium A supplemented with 5% FCS; FuGENE 6 was used as the transfection agent. For each transfection, the total amount of DNA was adjusted to 2.7 μg/dish by the addition of pcDNA mock vector. On day 3, cells were washed once with PBS and then switched to hydroxypropyl-β-cyclodextrin-containing medium B for 1 h. The cells were washed with PBS and then incubated with medium C containing either 30 μM cholesterol complexed with methyl-β-cyclodextrin or 1 μg/ml 25-hydroxycholesterol (delivered in ethanol, final concentration of 0.1%) as indicated. After incubation for 4 h, the cells were harvested, and the isolated nuclear and membrane fractions were subjected to immunoblot analysis with 0.2 μg/ml anti-HSV (SREBP-2), 5 μg/ml IgG-4H4 (Scap), or 1 μg/ml anti-Myc IgG-9E10 (Insig). Films were exposed for 8–20 s. *B*, [^{3}H]cholesterol binding to WT and Y234A mutant version of His_6-Scap(Loop1). Each reaction, in a final volume of 100 μl of buffer C with 0.004% Nonidet P-40 and 0.001% Fos-choline 13, contained 5 pmol of purified WT and Y234A mutant version of His_6-Scap(Loop1), 1 μg of bovine serum albumin, and the indicated concentration of [^{3}H]cholesterol (222×10^3 dpm/pmol) in the absence or presence of 10 μM unlabeled cholesterol. After 4 h at room temperature, the bound [^{3}H]cholesterol was measured as described under "Experimental Procedures." Each data point is the average of duplicate assays and represents specific binding after subtraction of blank values determined in the presence of unlabeled cholesterol. *C*, tryptic digestion of WT and Y234A mutant version of full-length Scap transfected into Scap-deficient hamster cells. SRD-13A cells were transfected with the indicated full-length pCMV-Scap plasmid and harvested for preparation of membranes as described under "Experimental Procedures." Aliquots of the 20,000 $\times$ *g* membrane fractions (100 μg) were incubated for 20 min at room temperature with 50 μM cholesterol complexed with methyl-β-cyclodextrin, followed by sequential treatments with 14 μg/ml trypsin (30 min at 30 °C) and 4000 units/ml peptide *N*-glycosidase F (4 h at 37 °C). The samples were then subjected to immunoblot analysis with 5 μg/ml anti-Scap IgG-4H4. The film was exposed for 30 s. *D*, immune detection of Scap·Insig-1 complexes. On day 2, SRD-13A cells were cotransfected with pCMV-Insig1-Myc together with either full-length pCMV-Scap or its mutant Y234A version as indicated. On day 3, the cells were incubated for 1 h with 1% hydroxypropyl-β-cyclodextrin, after which they received fresh medium containing one of the following sterols: none (−), 30 μM cholesterol complexed with methyl-β-cyclodextrin (*Chol*), or 1 μg/ml 25-hydroxycholesterol (*25HC*). After incubation at 37 °C for 4 h, each detergent-solubilized whole cell lysate was incubated with anti-Myc beads, followed by washing and elution with Myc peptide as described under "Experimental Procedures." The eluates were subjected to immunoblot analysis with either 5 μg/ml anti-Scap IgG-4H4 or 1 μg/ml anti-Myc IgG-9E10. Films were exposed for 3–5 s.

luciferase reporter assay (Fig. 5). It is possible that crucial cholesterol-binding residues could be identified by substituting amino acids other than alanine. Definitive identification of the cholesterol-binding site would be revealed if the structure of the loop could be determined by x-ray crystallography. Studies along these lines are under way.

In our [^{3}H]cholesterol-binding assays with recombinant Scap(Loop1), we used detergent concentrations that are at the borderline for micelle formation (0.004% Nonidet P-40 plus 0.001% Fos-choline 13). Moreover, we washed the nickel column and eluted the protein with solutions that lacked detergent. These conditions were determined empirically to produce an optimal ratio of specific to nonspecific [^{3}H]cholesterol binding. Under these conditions, we estimated that at saturation, 1 mol of [^{3}H]cholesterol bound to 4–5 mol of Scap(Loop1). Inasmuch as Scap(Loop1) behaved as a tetramer by gel filtration, the binding stoichiometry raises the possibility that 1 mol of tetramer binds 1 mol of cholesterol. In experiments not shown, we subjected cholesterol-bound Loop 1 to gel filtration, and the protein continued to behave as a tetramer. We therefore believe that cholesterol binding does not alter the tetrameric state. We have

no data as to the oligomerization state of Scap in ER membranes. Such studies are currently in progress.

Inasmuch as the crucial residue at position 234 is a tyrosine, we considered the possibility that the hydroxyl group must be phosphorylated or otherwise modified in order for Scap to exit the ER. This possibility was excluded when we substituted phenylalanine for tyrosine 234 in full-length Scap and found that this protein reached the Golgi normally (data not shown).

We also considered the formal possibility that Scap(Y234A) was simply failing to fold properly and was retained in the ER through the unfolded protein response. Several observations argued strongly against this possibility: 1) Scap(Y234A) showed the appropriate cleavage patterns for the cholesterol-bound configuration when treated with trypsin (Fig. 7*C*); 2) Scap(Y234A) bound to Insig-1 (Fig. 7*D*); and 3) Scap(Y234A) and WT Scap had similar half-lives as revealed by the rate of decline of the proteins after protein synthesis was inhibited with cycloheximide (supplemental Fig. S3). If Scap(Y234A) were misfolded, it would be expected to be degraded more rapidly.

In earlier papers, we referred to the region of Scap containing transmembrane helices 2–6 as the "sterol-sensing domain" (24, 27). This nomenclature was based on the observation that evolutionarily related sequences are present in other membrane proteins that are postulated to interact with or be influenced by sterols. The other proteins include 3-hydroxy-3-methylglutaryl-CoA reductase an ER-bound enzyme whose degradation is accelerated by sterols (28, 29); NPC1, a protein involved in the transport of cholesterol from lysosomes to the ER and to the plasma membrane (30); and Patched, which is the receptor for Hedgehog, the only protein known to contain covalently bound cholesterol (31). In view of the current data showing that the cholesterol-binding site in Scap is located in Loop 1 and previous data showing that the TM2–6 segment of Scap is the Insig-binding domain (7, 18), we will henceforth refer to the TM2–6 segment as the Insig-binding domain (Fig. 1). We have not ruled out the possibility that the Insig-binding domain contains another sterol-binding site. We think this possibility is unlikely because our previous study of sterol binding to the entire TM1–8 region of Scap showed evidence of only a single class of binding sites, and this class has the same properties as the binding site in Loop 1. It is noteworthy that the corresponding TM2–6 segment of 3-hydroxy-3-methylglutaryl-CoA reductase binds to Insig in a sterol-dependent fashion (32). The roles of the corresponding transmembrane segment in NPC1 and Patched remain to be determined. However, recent biochemical and crystallographic studies showed that the initial sterol-binding site in NPC1 is not contained in the transmembrane segment but rather lies in the N-terminal domain of the protein, which, like Loop 1 of Scap, projects into the lumen of the lysosome (33, 34). The current studies add important insights into the mechanisms by which a membrane protein monitors the levels of cholesterol in cell membranes. Further studies of Loop 1 of Scap promise to provide additional insights.

Acknowledgments—We thank our colleagues Nick Grishin, Hans Deisenhofer, and Dan Rosenbaum for helpful comments; Dorothy Williams and Arjun Raman for excellent technical assistance; and Lisa Beatty, Shomanike Head, and Muleya Kapaale for invaluable help with tissue culture.

REFERENCES

1. Radhakrishnan, A., Ikeda, Y., Kwon, H. J., Brown, M. S., and Goldstein, J. L. (2007) *Proc. Natl. Acad. Sci. U.S.A.* **104,** 6511–6518
2. Sun, L. P., Seemann, J., Goldstein, J. L., and Brown, M. S. (2007) *Proc. Natl. Acad. Sci. U.S.A.* **104,** 6519–6526
3. Horton, J. D., Goldstein, J. L., and Brown, M. S. (2002) *J. Clin. Invest.* **109,** 1125–1131
4. Goldstein, J. L., DeBose-Boyd, R. A., and Brown, M. S. (2006) *Cell* **124,** 35–46
5. Gong, Y., Lee, J. N., Lee, P. C., Goldstein, J. L., Brown, M. S., and Ye, J. (2006) *Cell Metab.* **3,** 15–24
6. Nohturfft, A., Brown, M. S., and Goldstein, J. L. (1998) *J. Biol. Chem.* **273,** 17243–17250
7. Yang, T., Espenshade, P. J., Wright, M. E., Yabe, D., Gong, Y., Aebersold, R., Goldstein, J. L., and Brown, M. S. (2002) *Cell* **110,** 489–500
8. Yabe, D., Xia, Z. P., Adams, C. M., and Rawson, R. B. (2002) *Proc. Natl. Acad. Sci. U.S.A.* **99,** 16672–16677
9. Sun, L. P., Li, L., Goldstein, J. L., and Brown, M. S. (2005) *J. Biol. Chem.* **280,** 26483–26490
10. Radhakrishnan, A., Goldstein, J. L., McDonald, J. G., and Brown, M. S. (2008) *Cell Metab.* **8,** 512–521
11. Brown, A. J., Sun, L., Feramisco, J. D., Brown, M. S., and Goldstein, J. L. (2002) *Mol. Cell* **10,** 237–245
12. Radhakrishnan, A., Sun, L. P., Kwon, H. J., Brown, M. S., and Goldstein, J. L. (2004) *Mol. Cell* **15,** 259–268
13. Goldstein, J. L., Basu, S. K., and Brown, M. S. (1983) *Methods Enzymol.* **98,** 241–260
14. Brown, M. S., Faust, J. R., Goldstein, J. L., Kaneko, I., and Endo, A. (1978) *J. Biol. Chem.* **253,** 1121–1128
15. Kita, T., Brown, M. S., and Goldstein, J. L. (1980) *J. Clin. Invest.* **66,** 1094–1100
16. Hannah, V. C., Ou, J., Luong, A., Goldstein, J. L., and Brown, M. S. (2001) *J. Biol. Chem.* **276,** 4365–4372
17. Ikeda, Y., Demartino, G. N., Brown, M. S., Lee, J. N., Goldstein, J. L., and Ye, J. (2009) *J. Biol. Chem.* **284,** 34889–34900
18. Yabe, D., Brown, M. S., and Goldstein, J. L. (2002) *Proc. Natl. Acad. Sci. U.S.A.* **99,** 12753–12758
19. Tessier, D. C., Thomas, D. Y., Khouri, H. E., Laliberté, F., and Vernet, T. (1991) *Gene* **98,** 177–183
20. Kapust, R. B., Tözsér, J., Copeland, T. D., and Waugh, D. S. (2002) *Biochem. Biophys. Res. Commun.* **294,** 949–955
21. Sakai, J., Nohturfft, A., Cheng, D., Ho, Y. K., Brown, M. S., and Goldstein, J. L. (1997) *J. Biol. Chem.* **272,** 20213–20221
22. Feramisco, J. D., Radhakrishnan, A., Ikeda, Y., Reitz, J., Brown, M. S., and Goldstein, J. L. (2005) *Proc. Natl. Acad. Sci. U.S.A.* **102,** 3242–3247
23. Nohturfft, A., Yabe, D., Goldstein, J. L., Brown, M. S., and Espenshade, P. J. (2000) *Cell* **102,** 315–323
24. Hua, X., Nohturfft, A., Goldstein, J. L., and Brown, M. S. (1996) *Cell* **87,** 415–426
25. Rawson, R. B., DeBose-Boyd, R., Goldstein, J. L., and Brown, M. S. (1999) *J. Biol. Chem.* **274,** 28549–28556
26. Yamamoto, T., Davis, C. G., Brown, M. S., Schneider, W. J., Casey, M. L., Goldstein, J. L., and Russell, D. W. (1984) *Cell* **39,** 27–38
27. Nohturfft, A., Brown, M. S., and Goldstein, J. L. (1998) *Proc. Natl. Acad. Sci. U.S.A.* **95,** 12848–12853
28. Gil, G., Faust, J. R., Chin, D. J., Goldstein, J. L., and Brown, M. S. (1985) *Cell* **41,** 249–258
29. Skalnik, D. G., Narita, H., Kent, C., and Simoni, R. D. (1988) *J. Biol. Chem.* **263,** 6836–6841
30. Pentchev, P. G., Vanier, M. T., Suzuki, K., and Patterson, M. C. (1995) in

The Metabolic and Molecular Basis of Inherited Disease (Scriver, C. R., Beaudet, A. L., Sly, W. S., and Valle, D., eds) McGraw-Hill Book Co., New York
31. Porter, J. A., Young, K. E., and Beachy, P. A. (1996) *Science* **274,** 255–259
32. Sever, N., Song, B. L., Yabe, D., Goldstein, J. L., Brown, M. S., and DeBose-Boyd, R. A. (2003) *J. Biol. Chem.* **278,** 52479–52490
33. Infante, R. E., Abi-Mosleh, L., Radhakrishnan, A., Dale, J. D., Brown, M. S., and Goldstein, J. L. (2008) *J. Biol. Chem.* **283,** 1052–1063
34. Kwon, H. J., Abi-Mosleh, L., Wang, M. L., Deisenhofer, J., Goldstein, J. L., Brown, M. S., and Infante, R. E. (2009) *Cell* **137,** 1213–1224
35. Wei, J. H., and Seemann, J. (2009) *Nat. Protoc.* **4,** 1653–1662